M.S. UDDIN*#, Y.W. LIU*, S. SHANKAR**

A NEW STAR-LIKE SURFACETEXTURE FOR ENHANCED HYDRODYNAMIC LUBRICATION PERFORMANCE

This paper presents a numerical modelling and optimization of a new 'star-like' geometric texture shape with an aim to improve tribological performance. Initial studies showed that the triangle effect is the most dominant in reducing the friction. Motivated with this, a 'star-like' texture shape consisting of a series of triangular spikes around the centre of the texture is proposed. It is hypothesised that by increasing the triangular effect on a texture shape, the converging micro-wedge effect is expected to increase, hence increasing the film pressure and reducing the friction. Using the well-known Reynolds boundary conditions, numerical modelling of surface texturing is implemented via finite difference method. Simulation results showed that the number of apex points of the new 'star-like' texture has a significant effect on the film pressure and the friction coefficient. A 6-pointed texture at a texture density of 0.4 is shown to be the optimum shape. The new optimum star-like texture reduces the friction coefficient by 80%, 64.39%, 19.32% and 16.14%, as compared to ellipse, chevron, triangle and circle, respectively. This indicates the potential benefit of the proposed new shape in further enhancing the hydrodynamic lubrication performance of slider bearing contacts.

Keywords: surface texturing; friction; film pressure; numerical modelling; Reynods equation

1. Introduction

Surface texturing has proved as a means to improve tribological performance of two bearing slider surfaces. By creating additional micro-hydrodynamic pressure effect and entrapping worn particles into the micro-dimples, the friction and wear between the underlying surfaces are significantly reduced. Typical applications of surface texturing are mechanical seals, piston-cylinder couples, and artificial implants. In the past, enormous research has been put forward to understand and evaluate the effect of different texture shapes, e.g. circle, ellipse, triangle and chevron, on their beneficial effects, e.g. [1]. With the choice of appropriate geometric dimension and environmental conditions, these basic texture shapes are shown to exhibit an improved lubrication characteristic as opposed to non-textured surface. However, they may not be the optimum shapes providing the best performance as desired in many applications. Therefore, a new design of geometric texture shape is sought, which will outperform the basic shapes.

The effect of surface texturing on improving the tribological performance can depend on shape, density, depth and pattern of dimples [2]. In this regard, ddifferent researchers reported different optimum texture geometries, indicating that there are still some gaps in understanding the effect of surface texturing. For instance, Yan et al. [3] suggested that the dimple area density was the most important geometrical parameter, followed by the dimple depth and the dimple diameter. In a tribological study on piston ring/cylinder liner contact, Rahmani et al. [4] investigated and optimised negative and positive type texture with different shapes in hydrodynamic lubrication. They concluded that the increase of textures on the bearing surface is beneficial and reiterated the similar observations of Yan et al. [3].

Yu et al. [5] found that the texture orientation with respect to the sliding direction has a significant influence on the load bearing capacity. As compared to the circle and the triangle, the ellipse shape orientated perpendicular to the sliding direction is found to achieve the highest load bearing capacity. Similar improvement was reported by Qiu et al. [6] and Yuan et al. [7]. It is however to be noted that the results are valid for sliding contacts with compressible fluid medium. Kim et al. [8] concluded that the effect of aspect ratio of texture shape on the friction reduction is dominant while the texture density has a marginal influence. Fabricated by laser surface texturing technique, Cho and Choi [9] reported that the friction of the textured surface decreases regardless of the texture density and the aspect ratio and the optimum texture density and the depth for all the sliding conditions studied were found to be 25% and 25 µm, respectively. Further, the benefit of micro-textured patterns applied on the artificial hip/knee joint components was reported by Chyr et al. [10].

Starting with an arbitrary shape with the aid of sequential quadrilateral programming, Shen and Khonsari [11] studied the optimization of the texture shape and found that the optimum shape for unidirectional and bidirectional sliding becomes the

*   SCHOOL OF ENGINEERING, UNIVERSITY OF SOUTH AUSTRALIA, MAWSON LAKES, SA 5095, AUSTRALIA
**   DEPARTMENT OF MECHATRONICS ENGINEERING, KONGU ENGINEERING COLLEGE, ERODE, TAMILNADU, INDIA
#   Corresponding author: Mohammad.Uddin@unisa.edu.au

1864

chevron and the trapezoid-like shapes, respectively. However, the optimum shapes are valid when the area ratio is of about 30% and the benefits disappear when the area ratio is higher than 30%. Very recently, Zhang et al. [12] reported that square texture pattern exhibits the best hydrodynamic effects, followed by the triangle, circle and rectangle. It was shown that when the apex of the triangle texture is aligned with the fluid flow direction, the converging wedge effect is maximized, resulting in an increase of hydrodynamic pressure lift and the decrease of friction. Syed and Sarangi [13] investigated the orientation effect on triangular and elliptical shapes and reported the similar benefits of the triangular texture.

It is clearly evidenced from the above literature review that the tremendous research effort has been made to realize the benefits of surface texturing. Very importantly, most of the studies in literature focused only on the basic regular shapes and attempted to optimize their geometries to achieve the best lubrication performance. It can be expected that there would be a new texture shape that may supersede the current basic shapes. To the best knowledge of the authors, however, there is no study so far focusing on a new texture shape different from basic regular shapes and its optimization to leverage the potential benefits. To address the above, this paper proposes a new 'star-like' texture shape by utilizing the converging wedge effect of the triangular shape. Parametric study by varying different geometries of the new shape was performed to evaluate the lubrication performance in terms of the film pressure and the friction coefficient. The shape was then optimized and compared with the basic regular shapes to justify the efficacy of the proposed shape.

2. Materials and method

2.1. Numerical modelling

The mechanical bearing sliders considered in this paper are schematically illustrated in Fig. 1(a). It is composed of a stationary textured wall and a moving smooth wall with a relative speed U in the x-direction. The textured surface consists of an array of micro dimples, as shown in Fig. 1(b). Each surface texture is assumed to be located at the centre of an imaginary square cell of sides $2r_1 \times 2r_1$, whereby, the centre of the imaginary square cell is the origin of the Cartesian coordinates (x, y). A Newtonian viscous fluid film separates the slider surfaces with a constant film thickness of h_o and a viscosity of μ. Each texture is assumed to have a depth from the top surface and the maximum texture depth is indicated as h_T (see Fig. 1(a)). Therefore, the film thickness for the texture varies along the imaginary cell and is given by:

$$h(x,y) = \begin{cases} h_o & \text{outside the surface texture} \\ h_o + h_T & \text{intside the surface texture} \end{cases} \quad (1)$$

The following assumptions are made for the theoretical model: (*a*) the lubricant is Newtonian and incompressible and its properties are constant throughout the slider contacts, (*b*) the temperature and the inertial effects are neglected, (*c*) there is no slip at the boundaries and (*d*) the fluid flow is laminar. The hydrodynamic lubrication regime is assumed to exist between the surfaces and no asperity contacts between the surfaces are assumed; therefore, no squeeze effect is considered in this study. With these assumptions, Reynolds equation is valid for the mechanical bearing couple modelling and its steady-state two-dimensional form can be expressed as:

$$\frac{\partial}{\partial x}\left(h^3 \frac{\partial P}{\partial x}\right) + \frac{\partial}{\partial y}\left(h^3 \frac{\partial P}{\partial y}\right) = 6\mu U \frac{\partial h}{\partial x} \quad (2)$$

where, x and y represent the global Cartesian coordinates, h is the local film thickness, P is the local film pressure. In this study, the effect of texture geometric shape and orientation is studied by estimating the film pressure and the friction coefficient over a single imaginary cell because the introduction of a pattern of dimples or textures on the entire bearing surface will provide qualitatively a similar trend [5]. By specifying the film thickness distribution, the operating parameters and the appropriate boundary conditions, Eq. (2) can be solved for the pressure distribution over the imaginary square unit cell.
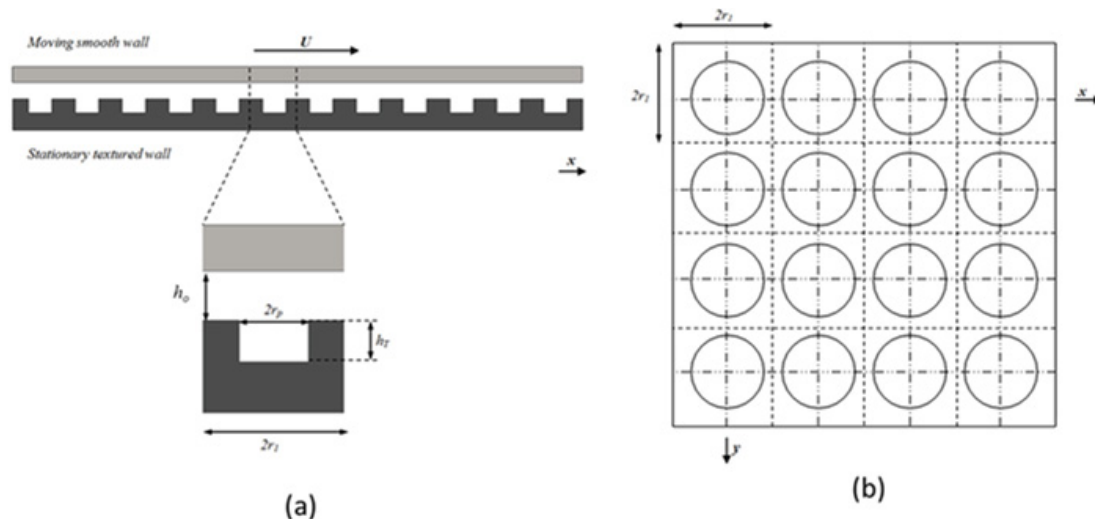

Fig. 1. Definition of slider surfaces with textures

Parameters used in numerical modelling

Parameter	Value
Imaginary cell length ($2r_1$)	100 μm
Minimum film thickness (h_o)	0.1 μm
Ambient pressure (P_o)	0.1 MPa
Cavitation pressure (P_c)	0.05 MPa
Fluid viscosity (μ)	0.0025 Pa-s
Sliding speed (U)	1.5 m/s
Maximum texture depth (h_T)	5 μm

At the surface texture boundary, the cavitation condition was approximated using Reynolds conditions, with the assumptions that the pressure gradient with respect to the direction normal to the boundary is zero and the pressure inside the cavitation is approximately zero. The Reynolds equation was solved using a five point grid finite difference method. The discrete form of the Reynolds equation was solved using the Successive Over Relaxation (SOR) Gauss-Seidel iterative method, in which, the film pressure at each node was computed with an over relaxation factor, ɔ, of 1.6, as Kang et al. [14] reported ɔ to be between 1.5 to 1.85, to accelerate the convergence. The convergence of the solution was checked with the relative error criterion, α, with the maximum variation in the average film pressure between two successive iterations to be less than 10^{-5}.

To determine the suitable square grid size or the number of nodes per imaginary cell, we have performed a mesh convergence study. We varied grid size from 10×10 (= 100 nodes/ cell) up to 150×150 (22,500 nodes/cell). For each grid size, we have estimated an average film pressure and average film thickness across the cell after achieving the convergence at each node via a series of iterations. It is found that the film pressure and film thickness fluctuate a lot at lower grid size. However, after the grid size of 100×100 up to 150×150, both become stable and the maximum fluctuation is found to be less than 0.04%, which is significantly small and can be considered negligible. As, higher the grid size, higher the computational cost. For instance, with the grid size of 150×150, it takes an average computational time of 370 seconds per iteration, as opposed to 80 seconds for the grid size of 100×100. As the grid size more than 100×100 does not provide any improvement in the accuracy of the results, the grid size of 100×100 is chosen in the numerical analysis presented in this paper. It must be noted that mesh convergence has been checked for texture shapes with different geometries and it is found that a grid size of 100×100 is sufficient to achieve the convergence while offering the acceptable accuracy. The key operating parameters used are shown in Table 1 and were kept constant throughout the study.

2.2. Defining basic texture shapes

Initially, four basic texture shapes – circle, ellipse, triangle and chevron, with flat bottom profile were considered to determine the shape which influences the most the lubrication performance. The geometric definition of the shapes along with the expressions of surface texture density, S_p, equivalent radius r_p and equivalent spacing between two slider surfaces can be found in [6].The film pressure and the friction coefficient for each texture shape were estimated as a function of surface texture density, S_p. S_p is defined as the ratio between the area of texture and the area of imaginary square cell. As the texture size gets bigger, S_p increases. Maximum S_p occurs when a side or edge of the texture touches the boundary of imaginary square cell. Note that based on the analysis of results of basic shapes, a new 'star-like' texture shape is proposed, which will be described in Section 4.

3. Results of basic texture shapes

Tribological performance of four basic shapes with flat bottom profile at a constant texture depth of 5 μm are simulated and compared. The aim of this analysis is at first to find out the optimum basic shape with an aim to maximize film pressure and minimize friction coefficient. The geometry of the optimum basic shape will then lead us to design the proposed texture shape which will outperform all the basic shapes. Fig. 2 shows non-dimensional average film pressure (P_a) as a function of texture density for four basic texture shapes. Non-dimensional average film pressure is defined as the ratio between the average of local film pressure across the cell and the atmospheric pressure. Plots to the right side of Fig. 2 show representative three-dimensional (3D) profiles of the pressure distribution along with the direction of sliding velocity with respect to the orientation of texture. As can be seen from Fig. 2, the triangle exhibits the highest film pressure among all. For the triangular shape, the film pressure increases with the increase of texture density; while it decreases for other shapes. The highest non-dimensional film pressure for the triangle reaches up to 7.75 at its maximum texture density of 0.8. This is due to the converging wedge effect of the triangle. As the sliding direction is towards the apex of the triangle, the fluid flow converges to the apex, hence resulting in an increase of hydrodynamic film pressure and separating two slider surfaces. The results are consistent with the findings of Sayed and Sarangi [13], which reported that negative triangle texture oriented along the direction of sliding showed the highest load bearing support. In contrary, such sharp converging effect is not existed in other texture shapes due to their inherent geometric characteristics.

One of the key indicators of the tribological performance due to texturing is the friction coefficient. Reducing the friction is thus considered the main focus to improve tribological characteristics of the sliding components (e.g. hip bearing couples). Figure 3 indicates the friction coefficient (f) profiles with the texture density. As can be seen from Fig. 3, the friction coefficient decreases slightly or maintains at a steady state level with the increase of the texture density. Interesting, the friction coefficient for the ellipse is significantly high at lower texture density (<0.2) and starts to decrease as the texture density increases and

1866

remains unchanged at the texture density between 0.5 and 0.8. Most importantly, the triangular shape exhibits the lowest friction coefficient among all the shapes at the texture density between 0.6 and 0.8. Higher texture density appears to be more beneficial in improving tribological performance. This clearly implies that as the film pressure increases, the friction coefficient decreases. The underlying mechanism for the decreased friction coefficient can be attributed to the similar reasons for the increased film pressure. Moreover, the results are hence quite in lined with the observation of Fig. 2.
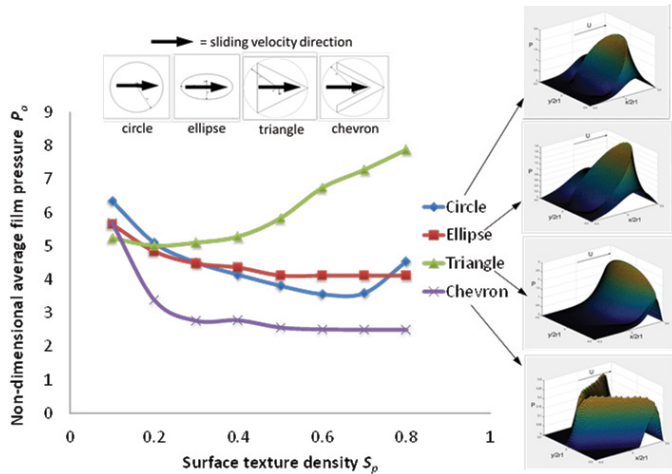
Fig. 2. Comparison of non-dimensional average film pressure between circle, ellipse, triangle and chevron
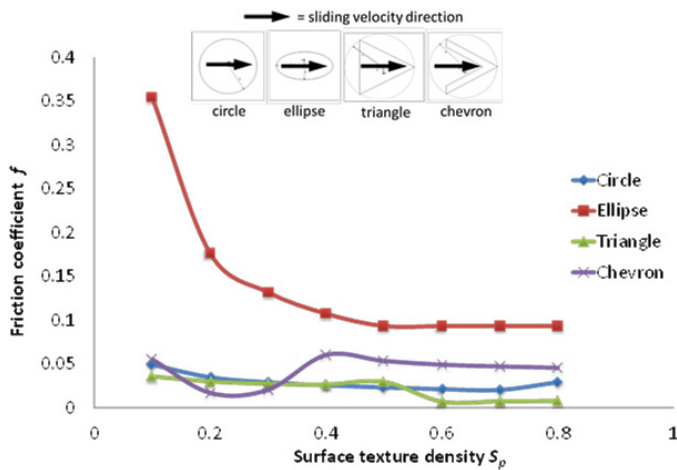

Fig. 3. Comparison of friction coefficient profile between circle, ellipse, triangle and chevron

4. Proposed 'star-like' texture shape

From the discussion in the previous section, it is revealed that the triangle offers the best lubrication performance among all four basic texture shapes. Using the beneficial effect of triangle geometry, we propose a new shape called 'star-like' texture shape, which consists of a number of apex points or triangular corners spaced at equally to each other. It is expected that, with having more triangles, the converging wedge effect of fluid flow

toward the apexes or the corners of the triangle will be further boosted, thus significantly increasing the film pressure or load bearing support and reducing the friction between the sliding surfaces. Fig. 4 shows an example of 'star-like' texture, in which, θ is defined as the apex angle of the corner, r_p is equivalent radius, γ is the orientation angle w.r.t. x-axis. $(x$-$y)$ is the Cartesian coordinate system and the origin of which is located at the centroid of the texture γ is zero degree when the x-axis passes through the apex of a triangle. It can be noted that the texture density of the proposed shape will increase with the increase of the number of apex points and decrease of apex angle, thus affecting the tribological performance. In order to determine the efficacy of the texture performance, the effect of texture geometries – the number of corner or apex points, the apex angle, and the orientation angle w.r.t. the sliding velocity on non-dimensional film pressure and friction coefficient is investigated.
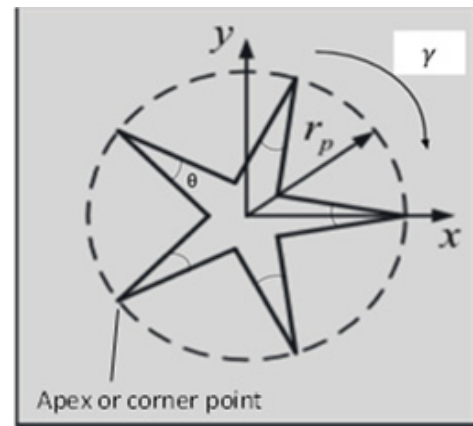

Fig. 4. Definition of the proposed 'star-like' texture shape (i.e. 5-pointed star texture)

By using a mesh size of 100×100 nodes and following the numerical modelling approach (as described in earlier section), star-like texture shapes with flat bottom profile at a maximum texture depth of 5 μm are simulated and compared.

5. Results of 'star-like' texture shape

5.1. Effects of the number of apex points

The effect of the number of apex or corner points on the film pressure was investigated. Fig. 5 shows the film pressure distribution profiles of 3-7 pointed star-like textures at the apex angle θ 5° and the orientation angle $\gamma = 0$°. It is seen that 4-pointed start texture reveals the highest hydrodynamic pressure as compared to all other shapes. The film pressure of 3, 4 and 7-pointed star shapes decreases as the texture density increases, while that of 5 and 6-point starts to increase after the texture density of about 0.2. Moreover, it is also clear that after the texture density of 0.6, the change of the film pressure is minimal; in other words, the film pressure tends to remain approximately unchanged with the increase of the texture density. It appears that the increase of the

number of the apex points of more than 4 does not necessarily increase the film pressure; instead starts to decrease. One possible reason would be that having more number of apex points increases the effective texture area which causes the film pressure to decrease. It may be possible that if a single apex of the triangle is aligned along with the fluid flow direction, the wedge effect is significant enough to lift the film pressure.
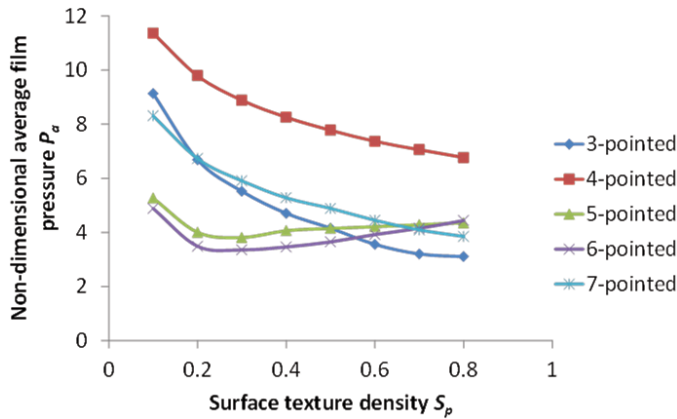
reduce the friction significantly, we varied the apex angle θ for a 6-pointed texture at an orientation angle γ of 0°. Fig. 7 shows non-dimensional average film pressure with respect to the apex angle. It is seen that the apex angle has insignificant effect on the film pressure until the texture density of 0.5. However, the film pressure increases notably with the increase of the apex angle after the texture density of 0.5.

Fig. 5. Effect of the number of apex points on non-dimensional average film pressure at the apex angle of 15° and the orientation angle of 0°
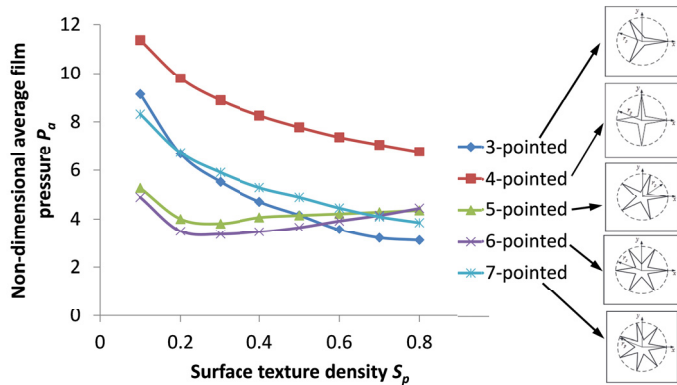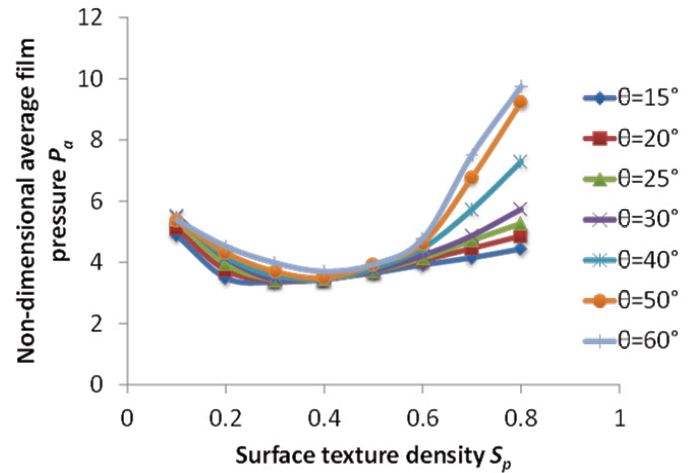

Fig. 7. Effect of the apex angle on non-dimensional average film pressure for a 6-pointed start texture at the orientation angle of 0°
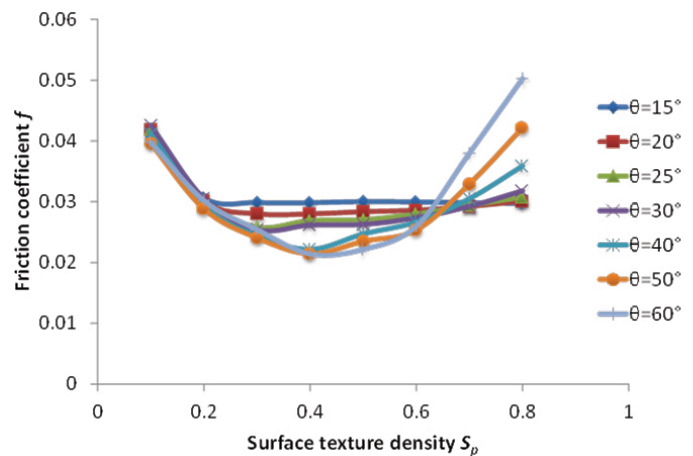

Fig.6. Effect of the number of apex points on the friction coefficient at the apex angle of 15° and the orientation angle of 0°

Fig. 8. Effect of the apex angle on the friction coefficient for a 6-pointed start texture at the orientation angle of 0°

Fig. 6 shows the friction coefficient profile of 3 to 7-pointed star-like textures at the apex angle θ 5° and the orientation angle $\gamma = 0$°. Overall, the friction coefficient decreases with the increase of the number of apex points. Interestingly, it is however to be noted from Fig. 6 that the 6-pointed texture exhibits the lowest friction coefficient among all other star-like textures. The result is quite in contradictory to the film pressure profile shown in Fig. 5. However, such result would be attributed to the fact that the film thickness might have increases across the texture as the number of the apex points increases, thus reducing the friction.

5.2. Effect of the apex angle

In this study, the effect of apex angle on the film pressure and friction was investigated. As 6-pointed texture appears to

It is clear that higher texture density and the apex angle essentially increase the converging wedge effect, causing the increase of the film pressure. However, it can be further hypothesized that the texture density would probably have a more dominant influence, than the apex angle, as the larger apex angle means the wider approaching area for the fluid flow towards the apex point and hence resulting in a lesser triangular converging effect. The friction coefficient profiles follow the same trend of the film pressure, as can be seen in Fig. 8, and the underlying mechanisms would be explained by the same reasons. For all the orientation angles, the friction coefficient is found to be minimum at the texture density of 0.4.

1868

5.3. Effect of the orientaton angle

Further, the influence of the texture orientation was investigated, in which, a 6-pointed star texture at the apex angle $\theta = 15°$ was studied by varying the orientation angle γ between 30° and 90°. The orientation angles of more than 90° were not studied as they will resemble the same effect in a cyclic manner. Only three texture density of 0.1, 0.15, and 0.2 were considered. Figs. 9 and 10 illustrate non-dimensional film pressure and friction coefficient profiles, respectively.
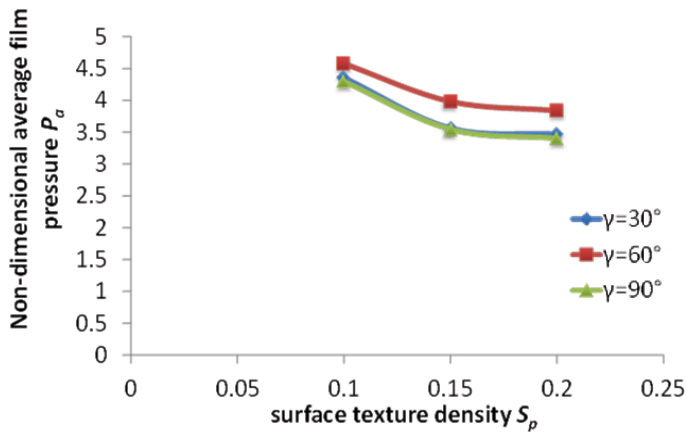

Fig. 9. Effect of the orientation angle on non-dimensional average film pressure for a 6-pointed star texture at the apex angle of 15°
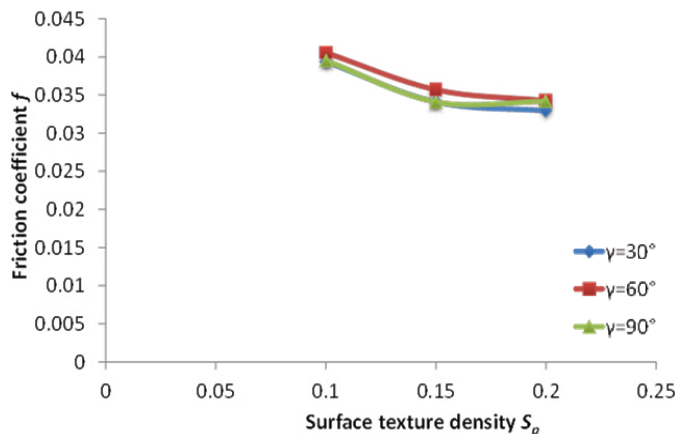

Fig. 10. Effect of the orientation angle on the friction coefficient for a 6-pointed star texture at the apex angle of 15°

It can be seen that the orientation angle of 60° shows the highest film pressure while the friction coefficient is negligibly affected by the orientation angle. It is expected that at the orientation of 60° more apex points are orientated towards the fluid follow and the converging wedge effect is further increased, hence increasing the pressure lift. Interestingly, both film pressure and friction coefficient follow the same trend qualitatively and quantitatively at the orientation angle of 30° and 90°. Overall, the film pressure and the friction coefficient, however, tend to slightly decrease with the texture density.

5.4. Optimization and comparison of 'star-like' shape with basic texture shapes

Results of film pressure and friction coefficient obtained from parametric study are compared with four basic textures shapes (circle, ellipse, triangle and chevron) and a search for the optimum texture shape is attempted. It is quite difficult to decide the optimum star-like texture as the best performance in terms of maximum film pressure and minimum friction coefficient does not occur at the same optimum texture geometry. However, as friction is often considered as the key indicator of lubrication performance of the sliding contacts, we aim to optimize the texture shape based on the analysis of friction coefficient results. Accordingly, a 6-pointed texture at texture density of 0.4 is apparently found to be the optimum shape and the apex angle θ of 15°-60° and the orientation angle γ of 30°-90° can be carefully selected. In order to further validate the effectiveness of the new texture, as a representative, we therefore have compared the friction coefficient of 6-pointed texture at the apex angle θ of 15° and the orientation angle γ of 60° with that of four basic shapes at texture density of 0.4. Fig. 11 shows a comparison of friction coefficient profile. It can be seen that though it is marginal, an improvement in friction reduction with 6-pointed star-like texture over the triangle shape is evident. For instance, the new optimum star-like texture reduces the friction coefficient by 80%, 64.39%, 19.32% and 16.14%, as compared to ellipse, chevron, triangle and circle, respectively.

All the results indicate that star-like textures with having more triangular geometries increase hydrodynamic pressure lift and minimize friction coefficient. As the new texture is geometrically simple in shape, it can be easily and accurately fabricated by the available manufacturing techniques, e.g. laser texturing. Hence the texture shape can be regarded as a potential texture candidate over the regular basic texture shapes to be used in the slider bearing surfaces to improve tribological performance and hence to increase service life of products.
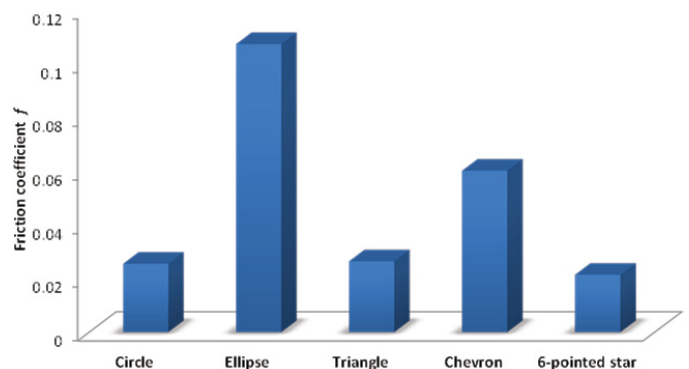

Fig. 11. Comparison of the friction coefficient between the optimum 6-pointed star texture with four basic shapes at texture density of 0.4

There are a number of limitations that may impact the current study presented in this paper. The parametric study of a new texture shape considered a constant texture depth, applied loading, sliding speed in numerical modelling. The variation of

these parameters however may influence the film pressure and friction coefficient results, and so does the optimum texture geometry obtained. This study focused on numerical modelling of a single texture within an imaginary square cell. Experimental validation is needed to justify the performance of the new shape as well as the underlying numerical modelling approach. It must be noted that with the given boundary conditions and parameters considered in the present numerical modelling, the results would be qualitatively valid and accurate. Translation of the results into new conditions may be explained with cautions. Future studies should take all other important parameters into account in the modelling to infer comprehensively the effectiveness of the new texture shape.

6. Conclusions

This paper presents a study of a new star-like surface texture for the improvement of hydrodynamic lubrication performance of parallel slider bearing surfaces. Preliminary results of four basic texture shapes indicate that the triangle texture outperforms among all in increasing the film pressure converging wedge effects of the triangles. The number of apex points of the new 'star-like' texture has significant effect on the film pressure and the friction coefficient, as compared to the apex angle and the orientation angle. A 6-pointed texture at a texture density of 0.4 is shown to be the optimum shape. The new optimum star-like texture reduces the friction coefficient by 80%, 64.39%, 19.32% and 16.14%, as compared to ellipse, chevron, triangle and circle, respectively. and the friction coefficient. Using the

beneficial triangular effect, a new 'star-like' texture shape consisting of a series of small triangles is proposed, with an expectation that the lubrication performance will be further boosted due to more.

REFERENCES

[1] I. Etsion, Y. Kligerman, G. Halperin, Tribol. Trans. **42**, 511-516 (1999).

[2] F. Meng, R. Zhou, T. Davis, J. Cao, Q.J. Wang, D. Hua, J. Liu, Appl. Surf. Sci. **256**, 2863-2875 (2010).

[3] D. Yan, N. Qu, H. Li, X. Wang, Tribol. Trans. **53**, 703-712 (2010).

[4] R. Rahmani, A. Shirvani, H. Shirvani, Applications and Future Trends. Woodhead Publishing, Cambridge, 470-517 (2010).

[5] H. Yu, H. Deng, W. Huang, X. Wang, Proc. Inst. Mech. Eng. Part J J. Eng. Tribol. **225**, 693-703 (2011).

[6] M. Qiu, B.R. Minson, B. Raeymaekers, Tribol. Int. **67**, 278-288 (2013).

[7] S. Yuan, W. Huang, X. Wang, Tribol. Int. **44**, 9, 1047-1054 (2011).

[8] B. Kim, Y.H. Chae, H.S. Choi, Tribol. Int. **70**, 128-135 (2014).

[9] M. M. Cho, H.J. Choi, Tribol. Lett. **56**, 409-422 (2014).

[10] A. Chyr, M. Qiu, J.W. Speltz, R.L. Jacobsen, A.P. Sanders, B. Raeymaekers, Wear **315**, 51-57 (2014).

[11] C. Shen, M.M. Khonsari, Tribol. Int. **82**, 1-11 (2014).

[12] Y.L. Zhang, X.G. Zhang, G. Matsoukas, Biosurface Biotribology **1**, 270-277 (2015).

[13] I. Syed, M. Sarangi, 16th National Conference on Machines and Mechanisms (iNaCoMM-2013), India, 850-856 (2013).

[14] S. Kango, D. Singh, P.K. Sharma, Meccanica **47**, 469-482 (2011).